Surface tailored electrospun polystyrene nanofiber membrane with TiO$_2$ nanoparticles for removal of copper ions from water

Santosh Wanjale[1,5,*], Mallinath Birajdar[1,2], Jyoti Jog[1], Ramesh Neppalli[3], Valerio Causin[3], József Karger-Kocsis[4], Jonghwi Lee[2], Prasad Panzade[5]

[1] Polymer Science and Engineering Division, National Chemical Laboratory

 Dr. Homi Bhabha Road, Pashan, Pune-411008, Maharashtra, India

[2] Department of Chemical Engineering & Material Science, Chung-Ang University, 221

 Heukseok-dong, Dongiak-gu, Seoul 15-756, South Korea.

[3] Dipartimento di Scienze Chimiche, Università di Padova, via Marzolo 1, 35131 Padova,

 Italy

[4] MTA–BME Research Group for Composite Science and Technology, Muegyetem rkp. 3, H-1111 Budapest, Hungary

[5] Aditya Birla Science & Technology Company pvt. Ltd. Tal. Panvel, Dist. Raigad 410208, Maharashtra, India

*Corresponding author: Santosh Wanjale

E mail   santosh.wanjale@adityabirla.com

Abstract

Novel Polystyrene (PS)/TiO$_2$ composite nanofiber membranes have been fabricated by electrospinning process for Cu^{2+} removal from water. The surface properties of the polystyrene nanofibers were modulated by introducing TiO$_2$ nanoparticles. The contact angle of the PS-based membranes decreased with increasing concentration of TiO$_2$, portray enhanced hydrophilicity. These membranes were highly effective in adsorbing Cu^{2+} ions from water and the adsorption capacity was found to be significantly higher (522 mg/g) than the results reported by other researchers. This was attributed to enhanced hydrophilicity and TiO$_2$ nanoparticles, which act as an effective adsorbent.

Key words: Electrospinning, TiO$_2$, Nanofiber, Metal ion adsorption, Water treatment/purification.

1. Introduction

Contamination of water by heavy metal ions have been a crucial problem to handle as it poses threat to public health. Many of these heavy metals including silver, copper, lead etc. are precious metals too and find variety of application with varied commercial values. Wide range of techniques, such as precipitation, coagulation, adsorption, ion exchange etc. have been employed to remove or recover these heavy metals. Out of these, adsorption process is more prevalent for heavy metal ions' removal, such as copper, cadmium, and zinc. However, the adsorption capacity, selectivity, regeneration is depend on material characteristics of the adsorbent. Nanoporous materials are not suitable for heavy metal removal because they could not be recycled easily. Compared with powder nanomaterials, mesoporous materials, electrospun membrane are good candidate because of ease of their high surface area and ease of modification [1].

Recently, electrospun nanofiber membranes became a subject of interest for removal of heavy metal ions. Electrospinning is a simple and versatile process by which polymer fibers with diameter ranging from few nanometers to several micrometers can be produced from a rich variety of materials that include polymers, composites and ceramics. Due to large surface area and high porosity of the related nanofibrous structure, these electrospun membranes exhibit high metal ion adsorption capacities compared with common fibrous filters [2]. Sang et al have demonstrated that electrospun chlorinated polyvinyl chloride can be used as absorption and filtration membranes to remove heavy metals from

groundwater [2]. Electrospun membranes of chitosan were found to be effective for adsorption of Cu^{2+} (485.4 mg/g) and Pb^{2+} ions (263.2 mg/g) from aqueous solutions [3]. Randomly oriented fibers of wool keratose/silk fibroin blend exhibited an exceptional good performance for the adsorption of metal ions and the performance was maintained even after several recycling cycles (desorption and re-adsorption) [4].

Further to improve the adsorption capacity of these membranes, methods like surface modification with functional groups –NH2, -SH, -SO$_3$H and incorporation of nanoparticles have been used. Ramakrishna et al. have reported the use of boehmite-nanoparticles-impregnated nylon membranes for removal of Cd^{2+} ions [5]. In another study Wei et al. showed the use of polyvinylidene fluoride-aliquat 336 fiber membranes for removal of cadmium from hydrochloric acid solutions [6].

In recent article, polyvinyl alcohol/SiO$_2$ composite nanofiber membranes functionalized with mercapto groups having mesostructure were demonstrated highest Cu^{2+} ion adsorption capacity (504.89 mg/g) than other reported nanofiber membranes [1]. In this article, materials were calcined at 500°C and the composite membranes were functionalized with mercapto groups. Li et al. prepared micrporous anatase TiO$_2$ nanofiber by calcination of PVP at 450°C in air for 3 hours to remove Cu^{2+} from water [7]. While carrying out search on metal ion adsorbing materials, we came across an article that described the adsorption properties of TiO$_2$. TiO$_2$ have been found a good adsorbent for removal of mercury, copper, lead and cadmium [8]. As most of the powder materials are not suitable for recycling and difficult to prepare a membrane. PS can employed as a substrate to give the strength and support to the TiO$_2$ nanoparticles to prepare membranes and this stimulated PS/TiO$_2$ membranes could be a potential alternative for removal of

heavy metal ions. In this article, it is revealed that there is no need of calcination and post functionalization of the composite membrane to improve the adsorption capacities. Here we present, simple, plain PS /TiO$_2$ composite nanofiber membrane that demonstrated to have better performance without further modification or functionalization.

2. Material and Methods

Polystyrene (PS) with an average molecular weight of 280.000 g/mol (GPC) and Titanium (IV) oxide (anatase-type nanopowder, particle size < 25nm, 99.70%, metal basis) were purchased from Aldrich chemicals. Copper sulphate CuSO$_4$. 5H$_2$O was purchased from SD-fine Chem. Limited, Mumbai. Dimethyl formamide (DMF,) used as solvent, was purchased from Merck Limited; Mumbai. De-ionized water was used for preparing aqueous solutions. All the chemicals were used as received without further purification.

2.1 Electrospinning

DMF solution of 10 wt.% PS was used after stirring for 24 hrs at room temperature (RT), after complete dissolution, three different concentrations (5%, 15% and 25%) of TiO$_2$ nanoparticles were added to PS solution at room temperature. These mixtures were ultrasonicated for 2 hrs at room temperature and composite fibers were coded with respect to the concentration of the TiO$_2$ nanoparticles into PS solutions i.e. PS, PS/TiO$_2$-5, PS/TiO$_2$-15 and PS/TiO$_2$-25 for 0, 5, 15 and 25% TiO$_2$ respectively.

Electrospinning is a unique method that produces polymeric fibers with diameter in the range of nano to a few microns using electrically driven jet of polymer solutions. Solution

was placed in a syringe of 10 ml with stainless steel hypodermic needle of inner pore diameter (0.8 mm) that act as an electrode. The syringe was filled with 8 ml of PS and PS/TiO$_2$ solution and then loaded in a syringe pump [Model 351, SAGE Instruments, Division of Orion Research, 11 Blackstone Street Cambridge, Mass.02139, USA)], to control a flow rate to maintain a constant size of droplet. The electrospinning apparatus consisted of a high voltage supply (0-40 kV), the syringe needle was connected to a high voltage generator [GAMMA High RR40 3.75/DDPM, Voltage regulated DC power supply; Ormond Beach, Florida 32174, USA] operated in positive DC mode. Aluminum plate, set in a closed chamber was used as grounded collector for fibers. Distance from needle tip to collector was fixed at 15 cm. The flow rate and an applied voltage were fixed at 0.015 ml/min and 15 kV respectively. The electrospinning was performed at room temperature.

2.2 Sample Characterization

2.2.1 Viscosity

Viscosity measurement was carried out using the Brookfield DV-II+ Prov, programmable viscometer [Brookfield Engineering Laboratories, INC. 11 Commerce Boulevard, Middleboro, MA 02346-1031 USA]. 1 ml solution was taken in the sample cup and the cone spindle (CPE-42). The measurements carried out at rpm 0.3 with shear rate 1.15 at 25ºC.

2.2.2 Conductivity

A Mettler Toledo SevenMulti [Mettler-Toledo GmbH, Analytical, Sonnenbergstrasse 74, CH-8603 Schwerzenbach, Switzerland] a digital & dual instrument with a provision to

measure the conductivity was used for conductivity measurements of the PS and PS/TiO$_2$ suspensions.

2.2.3 Scanning Electron Microscopy (SEM)

The morphology of the PS and PS/TiO$_2$ composite fibers samples were studied with a Leica Cambridge Stereo scan Model 440 scanning electron microscope (SEM) [Leica Microsystems, Wetzlar, Germany]. All specimens were gold coated prior to SEM characterization. EDAX was used for the elemental analysis.

2.2.4 X-ray Diffraction (XRD)

The structure of the PS/TiO$_2$ composite fibers samples were characterized using X-ray diffraction Philips 1830 [Almelo, The Netherlands]. X-rays of 1.5406 Å wavelength was generated by a Cu Kα source. The samples were scanned in the 2θ range of 3-80°

2.2.5 Small Angle X-ray Scattering (SAXS)

The SAXS patterns of the samples were recorded by MBraun system [Rivoli 10098 Italy], using a CuK$_α$ radiation from a Philips PW 1830 X-ray generator [Rivoli 10098 Italy]. The data were collected by a position sensitive detector and were successively corrected for blank scattering, desmeared and Lorentz-corrected.

2.2.6 Differential Scanning Calorimetry (DSC)

Differential Scanning Calorimetry (DSC) was performed using a model of DSC Q-10 Thermal Analysis [TA Instruments Division Waters Pvt Ltd. Bangalore, India]. Aluminum pans and lids were used for loading the samples. 5-7 mg of the nanofiber mat was used for analysis. The temperature range selected was between 0 and 200ºC. Tests were run under nitrogen flushing (50ml/min) at a heating rate of 10ºC/min.

2.2.7 Contact Angle Measurement

The wettability of the PS/TiO$_2$ composite fiber mats were characterized by using water sessile drop on Digidrop instruments (GBX) [225 Allee du Lyonnais 26300 Bourg-de-Peage, France]. Six measurements at different locations were averaged. The contact angle was measured using Image-J® software (National Institutes of Health, Bethesda, MD, USA, v1.48).

2.3 Metal adsorption studies

2.0 % (w/v) of solution was prepared by adding 5 g of CuSO$_4$.5H$_2$O into 250 ml of standard volumetric flask. De-ionized water was added up to the mark and used for adsorption study. 5 mg electrospun mats of pure PS and PS/TiO$_2$ fibers were weighed and soaked in the CuSO$_4$ solution for 5 min, 15 min, 30 min, 60 min and 1440 min. After the predetermined time, the solutions were filtered with Millipore filter and the solutions were characterized for UV absorbance at 780 nm. Adsorption experiments were performed on two electrospun mat samples. The concentration of metal ions in the solution was determined using UV-visible spectrophotometer and the adsorbed quantity was calculated using following equation (1).

$$Q = (C_0 - C_f).\frac{V}{M} \tag{1}$$

Where Q is the amount adsorbed (mg/g), C_0 and C_f are the initial and final concentrations (mg/L) of metal ion, V is the solution volume (L) and M is the amount (g) of adsorbent (i.e. nanofiber mat) used [9]. The concentration of metal ions was calculated with reference to the standard solution prepared. The desorption of Cu^{2+} ions from the surfaces of nanofibers was carried out using de-ionized water. The adsorbed mats were immersed in the de-ionized water for 1440 min. The fiber mats were removed from the solution and filtered. The absorbance of the respective metal solution was evaluated by UV-visible spectrophotometer [UV-1601(PC) S, Shimadzu Corporation, Kyoto, Japan] at the wavelength of 780 nm. The metal concentration of the solution was calculated using a standard calibration curve.

3. Results and discussion

3.1. Viscosity and conductivity of PS/TiO₂ suspensions

The viscosity and conductivity of the suspensions plays important role on the morphology and the diameter of electrospun nanofibers [10]. It has been found that as the viscosity increased, fiber diameter tends to increase and a beaded fiber may form. According to the literature [11], it is known that the charged ions present in the polymer solution have significant influence on the jet formation. In the processes of electrospinning, the ionic solutions develop increased charge to charge repulsion as the ionic concentration increases; hence, a higher tension is produced leading to the formation of Taylor cone, due to which fine and uniform nanofibers are formed. **Figure 1** Shows the viscosity and conductivity curves for PS/TiO₂ suspensions. The viscosity for pure PS solution was 84.7 mPa.s and for PS/TiO₂-5 it decreased from 84.7 to 42.0 mPa.s. The viscosity of suspensions was found to

be decreased with increase in concentration of TiO_2. The viscosity reduced from 84.7 mPa.s to 15.6 mPa.s for PS/TiO_2 with 25% TiO_2. As the ultrasonication is used for dispersing TiO_2 nanoparticles in the polymer solution it can break the chain length and thus the molecular weight and the other probable reason is that due to the plasticizing effect of TiO_2 that weakens the interactions between polymer chains.

3.2. Scanning Electron Microscopy analysis

Figure 2 shows the scanning electron microscopy (SEM) micrographs of pristine PS fiber and composites with 5, 15, and 25 wt% TiO_2. Pristine PS produced smooth and bead-free fibers. While after introduction of the TiO_2 nanoparticles into the PS matrix, the roughness of the fiber increased and the diameter of the fibers was influenced by the content of TiO_2 nanoparticles because the viscosity and conductivity play an important role on the morphology and the diameter of electrospun fibers [11]. Plain PS fibers had the largest diameter, i.e. 2.21 ± 0.5 μm. The fibers with 5, 15, and 25 wt% TiO_2 had diameters of 0.69 ± 0.3 μm, 0.98 ± 0.3 μm, and 1.65 ± 0.4 μm, respectively.

Figure 2. SEM micrographs and distribution of the diameters of the electrospun fibers of a) pure PS b) PS/TiO_2-5, c) PS/TiO_2-15, d) PS/TiO_2-25.

3.3. X –ray diffraction analysis

Fig. 3 shows the X-ray diffraction spectra of pure TiO_2 and PS/TiO_2 fibers. PS is an amorphous polymer, and as such it just yielded a featureless halo. The XRD pattern of TiO_2 shows five primary peaks at $25.7º$, $38.23º$, $48.2º$, $55.4º$ and $62.9º$ which are attributed to the

(101) (112), (201), (205) and (211) planes, respectively, of anatase crystalline phase. Recall that anatase is one of the polymorphs of TiO_2 [12-20]. Since the surface area of anatase phase is higher than the rutile phase it is preferred in most of the applications. The XRD diffraction patterns of the PS/TiO_2 fibers showed a superposition of the amorphous halo due to the PS matrix and diffraction of TiO_2 particles. It is notable that no changes in the breadth of the diffraction signals appeared, indicating that the TiO_2 nanoparticles were distributed in the PS matrix without forming any aggregates [21]. As seen in **Figure 3**, the intensity of such peaks increases with increasing TiO_2 content. It is also important to note that the anatase phase of TiO_2 did not change after producing the composite fibers via electrospinning.

Figure 3. X-ray Diffraction (XRD) of pure TiO_2 nanoparticles, pure PS mat, PS/TiO_2-5, PS/TiO_2-15 and PS/TiO_2-25 composite fibers.

3.4. SAXS analysis

It is utmost important to study the dispersion level of the TiO_2 nanoparticles in the PS matrix, as the dispersion level has the greatest impact on the viscosity and hence on the fiber morphology. SAXS provides structural information about heterogeneities, size, shape and intermolecular spacing within aggregate stacks. Thus SAXS was employed to get the knowledge on dispersion level, whether the TiO_2 nanoparticles are homogeneously dispersed or present in aggregates. The SAXS spectra of the TiO_2 containing fibers are shown in **Figure 4.** Note that fibers produced solely from PS gave a featureless SAXS signal.

Figure 4. SAXS spectra of the electrospun PS fibers containing the indicated amounts of TiO$_2$

The peaks displayed in **Figure 4** are indicative of a correlation between the inorganic particles, and through the Bragg equation it is possible to estimate the average distance between such particles, i.e. 31.1 nm, 23.2 nm, and 18.7 nm in the case of the fibers containing 5%, 15% and 25% TiO$_2$, respectively. This is clearly understood because, as shown in SEM micrographs, the diameter of the fibers did not reduce dramatically. Therefore particles must be accommodated in the same volume, with the result of lying closer together. By applying the Guinier equation (2) as given below [22], an estimation of the average size of the individual TiO$_2$ particles was possible, in all the fibers the radius of gyration of TiO$_2$ particles was 10 nm, in agreement with the size reported by the manufacturer, i.e. $<$ 25 nm. The average radius of gyration of TiO$_2$ particles was constant irrespective of the loading of the fiber, confirming that no coalescence was occurred.

$$\ln I(q) = \ln I(0) - \frac{R_g^2}{3} \cdot q^2 \qquad (2)$$

3.5. Thermal analysis

Introduction of nanoparticles also affects the matrix thermal properties. Therefore DSC was used to study the effect of introduction of TiO$_2$ nanoparticles on glass transition temperature (T$_g$) of PS. Thermal transitions of PS and PS/TiO2 composite fibers were measured by DSC, i.e. monitoring the heat flow vs. temperature. PS is non-crystalline and therefore does not exhibit any crystallization or melting transitions. After two cycles at 10 ºC/min, from 0 up to 200 ºC. The T$_g$ values of PS and composite fibers are presented in

figure 5 it was found that the T_g did not change significantly with the addition of TiO_2 nanoparticles. This result indicates that addition of TiO_2 does not significantly influence the mobility of PS chains in the solid state [23-25].

Figure 5. DSC thermal properties of PS polymer, pure PS mat, PS/TiO_2-5, PS/TiO_2-15 and PS/TiO_2-25 composite fibers.

3.6. Adsorption Kinetics
3.6.1. Adsorption studies
Figure 6 depicts the metal adsorption curves of PS/TiO_2 composites fibers. The result shows the adsorption by composites fibers gets equilibrated for 60 min and this may be due to adsorption and diffusion phenomena. Metal adsorption studies were carried out with different time duration but by the particular amount of thin fiber mats in decided amount and fixed concentration of solution, by taking absorbance before and after the metal adsorption. The metal adsorption studies were carried out using 2% w/v Cu^{2+} solutions. The fiber mats of PS/TiO_2 adsorbed more Cu^{2+} with increasing TiO_2 content in PS/TiO_2 fiber membrane. According to our expectation, fibers of PS/TiO_2 composite adsorbed more Cu^{2+} when compared to fibers of PS. Fibers of PS/TiO_2 composites exhibited higher Cu^{2+} ion adsorption capacity in comparison with previous studies of metal ion adsorption using electrospun nanofibers. This is due to the adsorbing nature of TiO_2 which also modify the PS fibre surface into hydrophilic.

Figure 6. Adsorption of Cu^{+2} of pure PS and PS/TiO_2-based nanofiber mat membranes (mg/g of mat) as a function of time.

As can be seen from **Figure 6** pristine PS does not play a role in adsorption phenomena of Cu^{2+}, while after addition of 5% TiO_2 its adsorption behavior was dramatically improved. This may be due the enhanced wettability of the surface which is significant in getting the Cu^{2+} ions adsorbed on the surface of fibers. Thus the wettability of the PS and PS/TiO_2 fiber mat was studied using the contact angle method.

3.6.2. Contact angle measurement

In case of the PS/TiO_2 series, the contact angle obtained for PS/TiO_2-5 to PS/TiO_2-25 changed from 84.4° to 40.7° as shown in **Figure 7.** Hence, the wettability of the TiO_2 loaded PS fiber mat surface increased as the TiO_2 content increased in PS. Thus PS substrate was demonstrated to have a profoundly hydrophobic behavior with a contact angle of 156.4°, which was lowered significantly to 40.7° by introduction of TiO_2 nanoparticles and lead to a deep wettability modulation. Wang et al. performed contact angle measurement of PS/TiO_2 hybrid membranes with different TiO_2 content and the results are in good agreement [26]. Surface wettability also depends on the roughness of the fibers [27-29]. When the surface roughness is high, only a small quantity of water can come into contact with the fiber surface, resulting in a large barrier interaction between water and air [30]. As a result, rough nanostructured surfaces yield materials with higher measured contact angles. TiO_2 nanoparticle loading generates rougher nanofiber surfaces; however, this effect appears to be masked by the hydrophilic effect of the TiO_2 nanoparticles. In conclusion, modulating the dynamic wetting profile of a PS substrate by impregnating TiO_2 nanoparticles a highly functional PS/TiO_2 substrate could be produced.

Figure 7. Contact angle measurements of pure PS mat, PS/TiO$_2$-5, PS/TiO$_2$-15 and PS/TiO$_2$-25 composite fibers.

3.6.3. Adsorption Kinetics

As per the figure 6, the adsorption was studied at various time periods like 5, 15, 30, 60 and 1440 minutes. Figure depicts that initially the adsorption rate is increased and then gets equilibrated after 60 minutes. The adsorption was inconsistent up to 60 minutes due to the composite fibers were in the process of diffusion and adsorption of copper to attain equilibrium.

The experimental data was analyzed using two kinetic models like pseudo – first order (eq.2) and pseudo – second order (eq.3). [7]

The pseudo – first order is expressed as follows

$$\log(q_e - q_t) = logq_e - \frac{k1}{2.303}t \tag{3}$$

Where q_e and q_t are the adsorption capacity at equilibrium and at time t, respectively (mg/g) k_1 is the rat constant of the pseudo first order adsorption. The values of log (q_e – q_t) were correlated with time t, (hrs.) This plot should give linear relationship from which k1 and qe can be determined from the slope and intercept, respectively as shown in figure 8.

The pseudo – second order adsorption kinetics rate equation is expressed in linear form as below.

$$\frac{t}{q_t} = \frac{1}{k_2 \, q_e^2} + \frac{1}{q_e}t \tag{4}$$

Where q_e and q_t are the adsorption capacity at equilibrium and at time t, respectively (mg/g) k_2 is the rat constant of the pseudo second order adsorption. The rate constant for pseudo second order equation can be determined from plot t/q_t vs. t as shown in figure 9.

The kinetics parameters obtained for both the models are given in table 1. The correlation coefficients values for pseudo second order model are much higher than that of pseudo first order model. While the experimental adsorption capacity values are very close to the calculated (from model equations) for PS/TiO$_2$ -5 and PS/TiO$_2$ – 15 for the pseudo second order model and higher for PS/TiO$_2$ – 25. It is also observed that experimental value and calculated value of the adsorption capacity for PS/TiO$_2$ – 25 are very close if the first order model is followed.

The sorption behaviors that we have observed helped to elucidate possible mechanisms involved in the sorption of Cu^{2+} ions on the PS/TiO$_2$ nanofibrous mats. We postulate that the sorption on the titanium ions-free mats was primarily driven by the complexation of Cu^{2+} ions with the free titanium ions in the TiO$_2$ as reported in previous study [8].

The adsorption and desorption process of the mat was repeated three times. It was observed that the adsorbed ions could be easily removed from the mat and the mat could be reused for adsorption of the Cu^{2+} ions. The exact amount of metal adsorbed by the material was calculated from the standard calibration curve of the metal salts. The percent desorption was calculated and it was found to be 90 %. The above results of adsorption and desorption confirm that these electrospun membranes are promising materials for removal of heavy metal ions.

3.6.4. EDAX analysis

The presence of Cu^{2+} ions on the surface of the PS/TiO$_2$ fiber mats was validated by Energy dispersive analysis of X-ray (EDAX). An analytical technique used for the identification and elemental analysis of samples. EDAX measurements show the distributions of Cu^{2+}

ions in the composite fiber mat surface. The EDAX mapping results are included in **Figure 10** (A) and (B). These elemental maps confirm the presence of Cu on the PS/TiO$_2$ composite fiber surface.

Figure 10 (A)

Figure 10 (B)

Figure 10 (**A**) EDAX compositional data of PS/TiO$_2$-25 composites after 1440 min of insertion in CuSO$_4$ solution; (**10 B**) EDAX mapping showing the presence of Cu^{2+} ions on the mat (note: red spots represent Cu)

4. Conclusion

In summary, electrospinning of PS/TiO$_2$ composites was carried out with the goal of preparing functional fibers for removal of metal ion contaminants from waste water. The adsorption capacity of the PS fiber mats with TiO$_2$ was found to be more effective for Cu^{2+} ion adsorption (522 mg/g) than other reported results. This is due to the deep wettability modulation of PS by impregnating TiO$_2$ nanoparticles and the adsorbing nature of TiO$_2$ nanoparticles. These results demonstrate that the wettability modulation is important to improve the performance of the fibers. Consequently this composite membrane can have a great potential to remove and recover heavy metal ions from contaminated waters.

Acknowledgements

References

[1] W. Shengju, L. Fengting, W. Yinan, X. Ran, L. Guangtao, Chem. Comm. 46 (2010) 1694-1696.

[2] L. Cunzhen, Li. Fasheng, C. Jiaqing, G. Qingbao S. Yimin, Desalination. 223 (2008) 349-360.

[3] H. Sajjad, P. Soo-Young, J. Membr. Sci. 328 (2009) 90-96.

[4] S. K. Chang, H. G. Eun, U. In Chul, H. P. Young, J. Membr. Sci. 302 (2007) 20-26.

[5] H. Garudadhwaj, B. Rajesh Kumar, W. J. Ng, S. Ramakrishna, J. Mater. Sci. 43 (2008) 212-217.

[6] B. T. Yen, L. K. Ilias, S. Wei, J. Mater. Sci. 44 (2009)1101-1106.

[7] D Vu, Z Li, H Zhang, W Wang, Z Wang, X Xu, B Dong, C Wang. J. Colloid Interface Sci. 367 (2012) 429-435.

[8] L.R. Skubal, N.K. Meshkov, J. Photochem. Photobio. A: Chem. 148 (2002) 211-214.

[9] S. Xiaoa, H. Mac, M. Shen, S. Wang, Q. Huang, X. Shi, Colloid. Surfac. A: Physicochem. Eng. Aspects. 381 (2011) 48-54.

[10] H. Mastumoto, a. Tanioka, Membranes 1 (2011) 249-264.

[11] E. Kostakova1, M. Seps, P. Pokorny, D. Lukas, eXPRESS Polym. Lett. 8 (2014) 554-564.

[12] B. Saba, H. Sadaf, A. S. Niyazi, A. Areqi, Ionics. 16 (2010) 239-244.

[13] L. Soo-Keun, W. C. Kyung, K. Sun-Geon, Aerosol. Sci. Techn. 36 (2002) 763-770.

[14] Z. Lijun, Y. Shanshan, T. Baozhu, Z. Jinlong, A. Masakazu, Mater. Lett. 60 (2006) 396-399.

[15] N. Norio, H. Toyoharu, J. Appl. Polym. Sci. 105 (2007) 3662-3672.

[16] C. Li, S. Haixia, L. Zhen, F. Cang, C. Su, W. Yanru, Collo. Polym. Sci. 285 (2007)1515-1520.

[17] M.A. Behnajady, N. Modirshahla, M. Shokri, B. Rad, Global nest J. 10 (2008) 1-7.

[18] A.E Deniz, A. Celebioglu, F. Kayaci, T. Uyar, Mater. Chem Phys. 129 (2011) 701-704.

[19] S.I. Shah, W. Li, C.P. Huang, O. Jung, C. Ni, Proceedings of the National Academy of Sciences, 99 (2002) 6482-6486.

[20] W. Li, S. Ismat, M. Shah, S. Sung, C.P. Huang, J. Vacu. Sci. Techn. 20 (2002) 2303-2308.

[21] V. Sesha Sai Kumar, K. Rao, Journal of Nano – and Electronic Physics, 5, (2013) 2026

[22] H. Peterlik, P.Fratzl, Monatshefte. Fur. Chemie. 137 (2006) 529-543.

[23] U. Tamer, H. Rasmus, H. Jale, Z. Xingfei, B. Flemming, K. Peter, Nanotechnology 20 (2009) 125605.

[24] P. W. Adam, T. N. Sonbinh, H. K. Jun, Nanoscope 6 (2009) 26-29.

[25] O. Nobuaki, SII Nanotechnology, TA-68. 1985.

[26] Y. Yang, P. Wang, Polymer 47 (2006), 47, 2683-2688.

[27] M.V. Jose, V.Thomas, K. T. Johnson, D. R. Dean, E. Nyairo, Acta Biomater. 5 (2009) 305-315.

[28] F. Yang, J. G. C. Wolke, J. A. Jansen, Chem. Eng. J. 137 (2008) 154-161.

[29] A. U. Zillohu, R. Abdelaziz, S. Homaeigohar, I. Krasnov, M. Muller, T. Strunskus, M. Elbahri, Scientific Reports 2014, 6.

[30] A. Marmur, Wetting on Hydrophobic Rough Surfaces: To Be Heterogeneous or Not To Be?, Langmuir 19 (2003) 8343-8348.

List of Tables

List of Figures

Figure 10. (**A**) EDAX compositional data of PS/TiO_2- 25 composites after 1440 min of insertion in $CuSO_4$ solution; (**B**) EDAX mapping showing the presence of Cu^{+2} ions on the mat (note: red spots represent Cu)

Figure 1. Viscosity and Conductivity of PS/TiO$_2$ suspensions containing pure (1) PS-10 & different amounts of TiO$_2$ in (2) PS/TiO$_2$-5, (3) PS/TiO$_2$-15 and (4) PS/TiO$_2$-25.
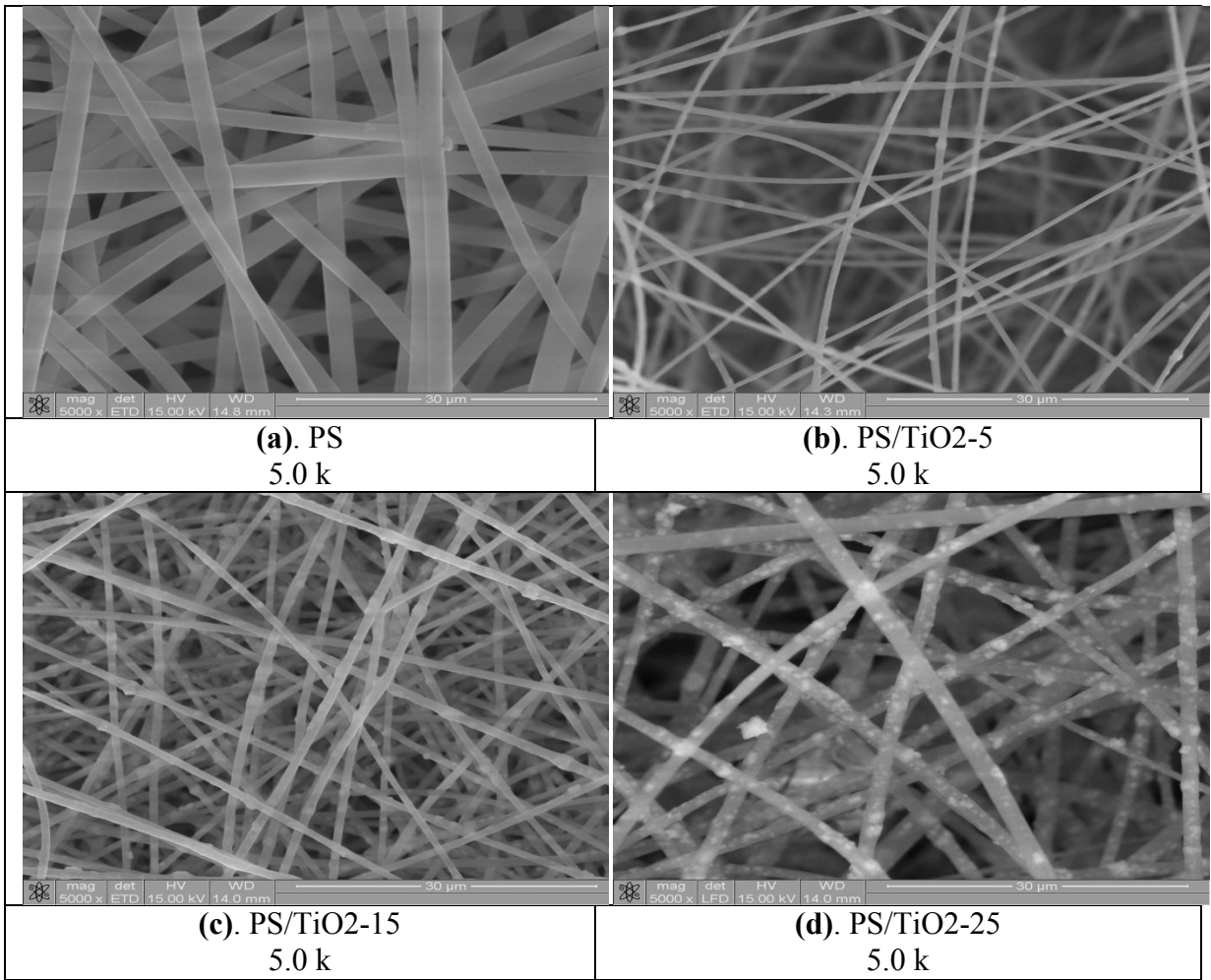
(a). PS 5.0 k	**(b)**. PS/TiO2-5 5.0 k
(c). PS/TiO2-15 5.0 k	**(d)**. PS/TiO2-25 5.0 k

Figure 2. SEM micrographs and distribution of the diameters of the electrospun fibers of

a) PS b) PS/TiO$_2$-5, c) PS/TiO$_2$-15, d) PS/TiO$_2$-25.
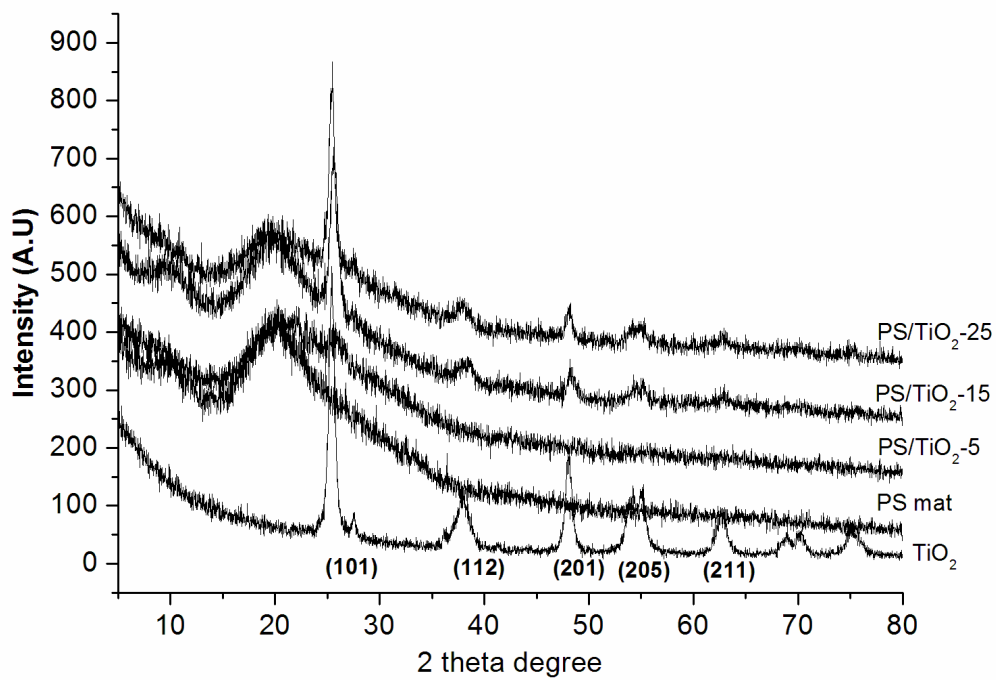
Figure 3. X-ray Diffraction (XRD) of pure TiO_2 nanoparticles, pure PS mat, PS/TiO_2-5, PS/TiO_2-15 and PS/TiO_2-25 composite fibers.
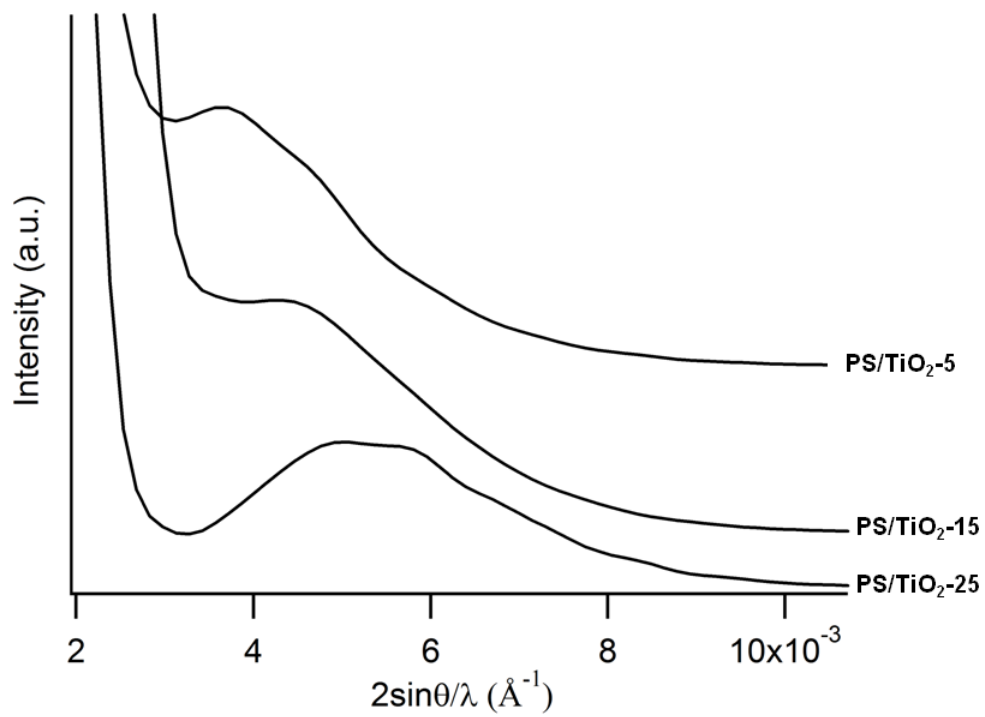
Figure 4. SAXS spectra of the electrospun PS fibers containing the indicated amounts of TiO$_2$
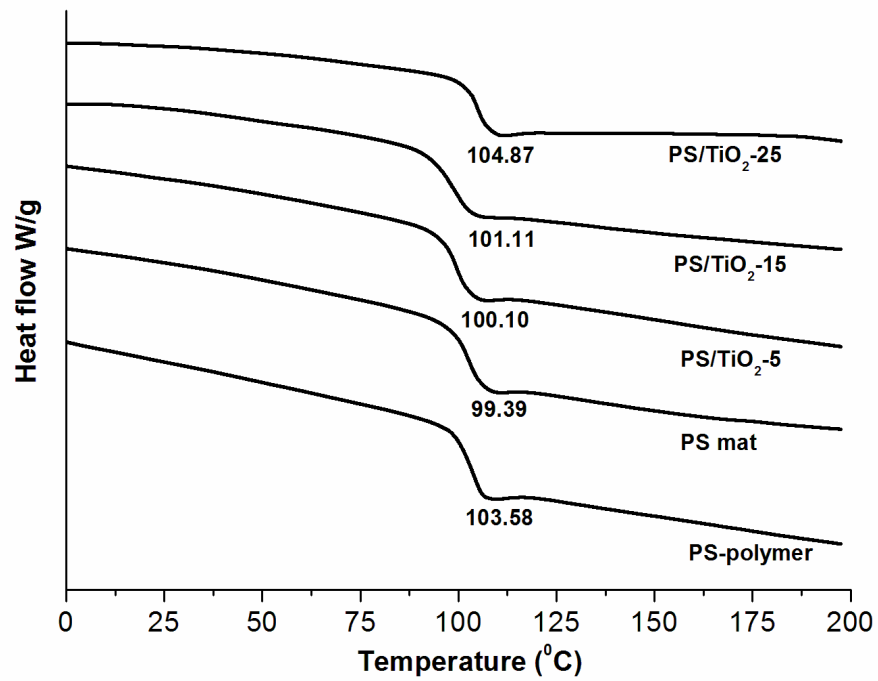
Figure 5. DSC thermal properties of PS polymer, pure PS mat, PS/TiO$_2$-5, PS/TiO$_2$-15 and PS/TiO$_2$-25.
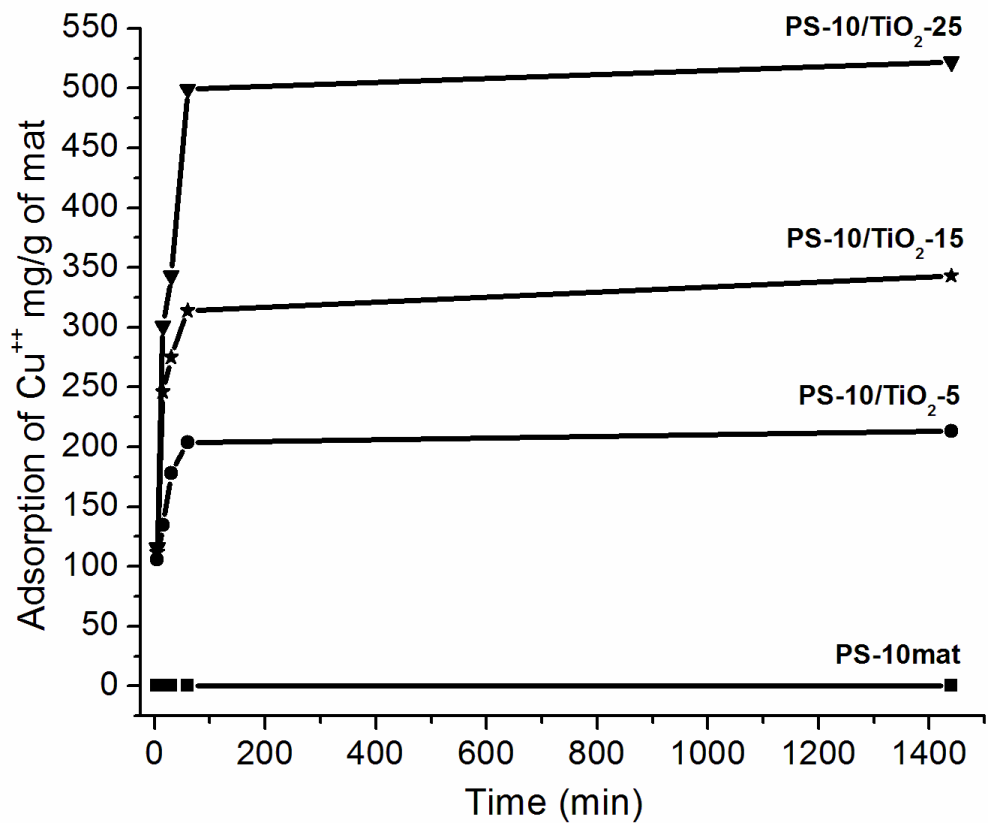
Figure 6. Adsorption of Cu^{2+} using PS and PS/TiO$_2$-based nanofiber mat membranes as a function of time.
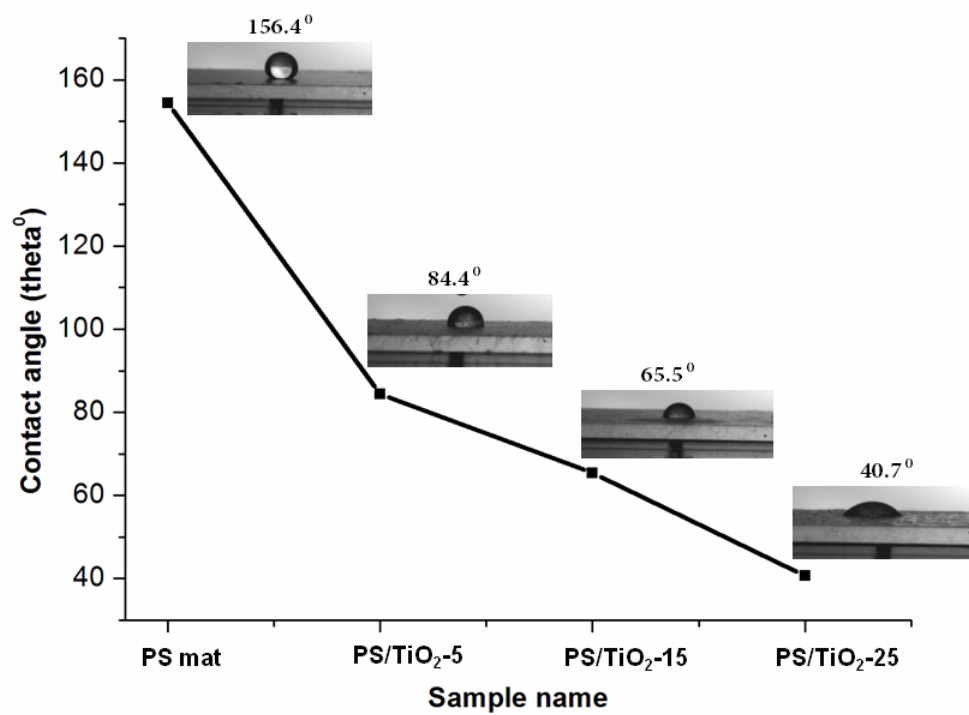
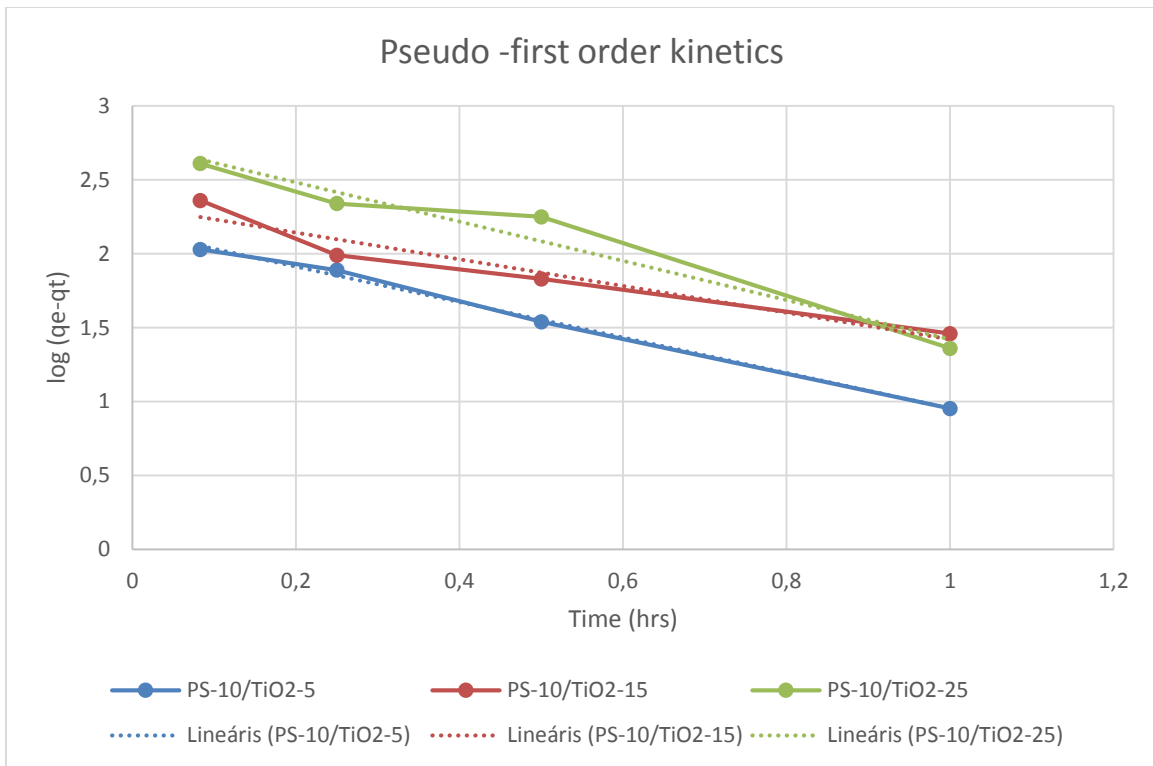**Figure 7.** Contact angle of PS mat, PS/TiO$_2$-5, PS/TiO$_2$-15 and PS/TiO$_2$-25.

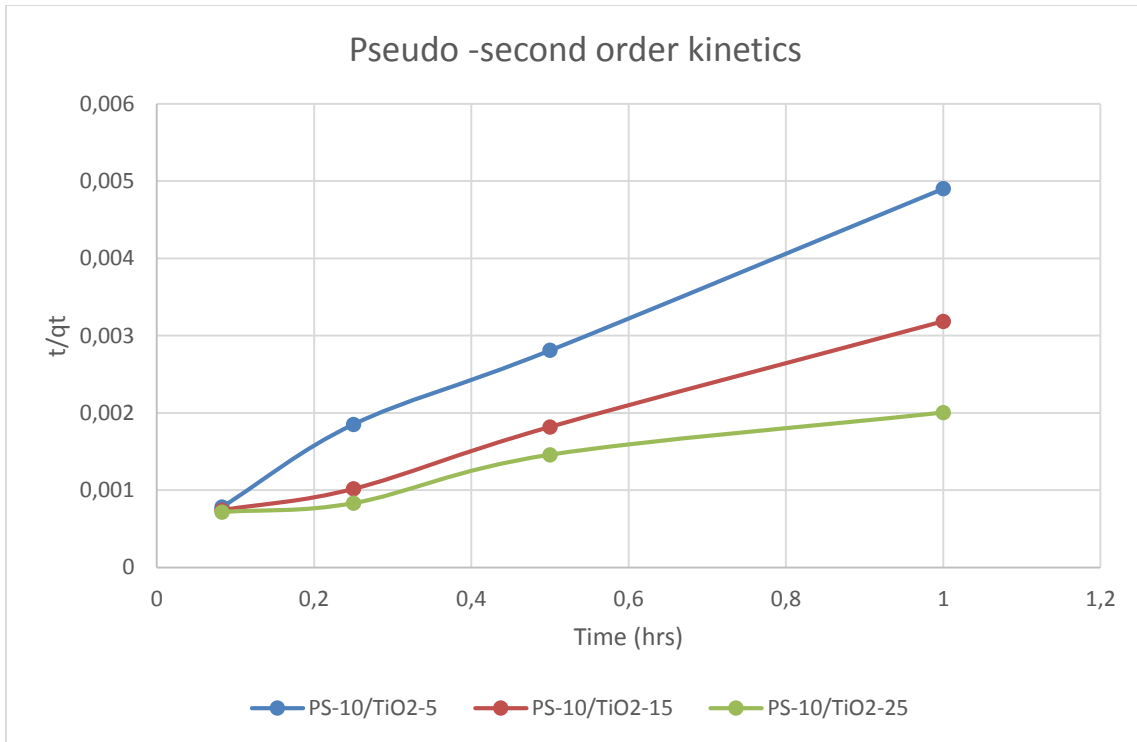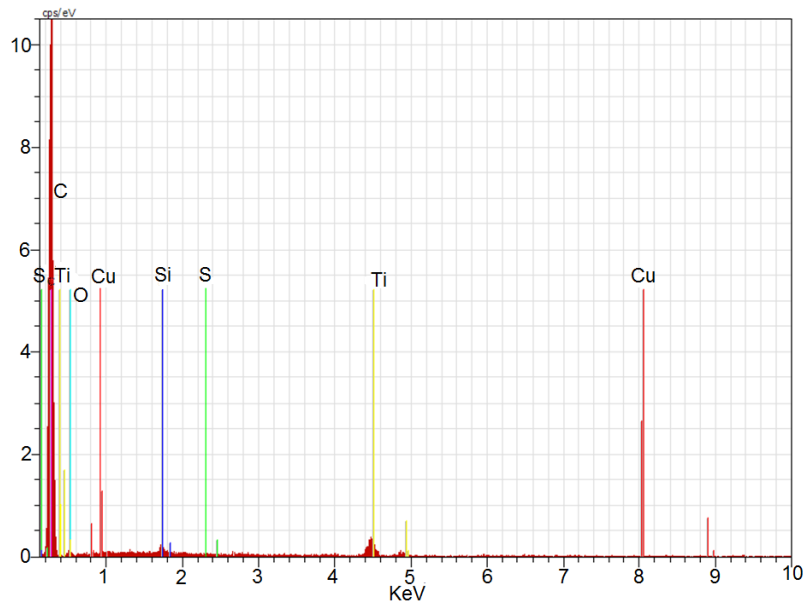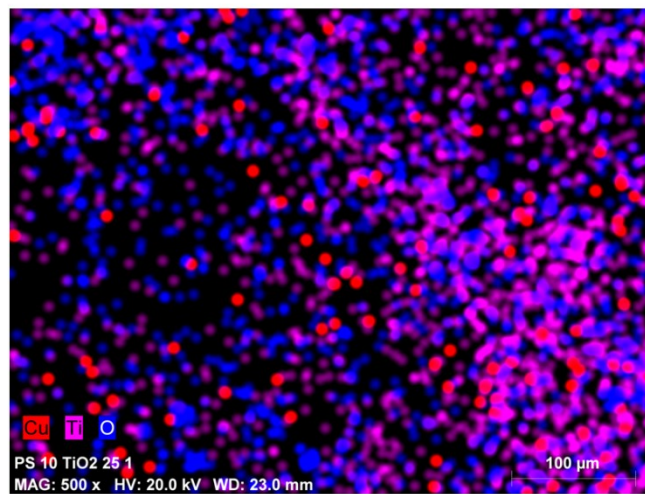**Figure 8.** Adsorption kinetics of Cu^{2+} using pseudo first order model

Figure 9. Adsorption kinetics of Cu^{2+} using pseudo second order model

(A)

(B)

Figure 10. (**A**) EDAX compositional data of PS/TiO$_2$- 25 composites after 1440 min of insertion in CuSO$_4$ solution; (**B**) EDAX mapping showing the presence of Cu^{+2} ions on the mat (note: red spots represent Cu)

Table 1.Kinetic parameters for adsorption of Cu^{2+} on PS/TiO_2 composite fibers

Sample	Pseudo first order model				Pseudo second order model		
	q_e, experimental (mg/g)	k_1	R^2	q_e, calculated (mg/g)	k_2	R^2	q_e, calculated (mg/g)
PS/TiO_2 -5	213	1.197	0.997	142	0.0044	0.993	227
PS/TiO_2 -15	343	0.903	0.935	211	0.0027	0.995	370
PS/TiO_2 -25	522	1.327	0.957	560	0.0015	0.966	667